

## EVIDENCE FOR BIMODAL FISSION IN THE HEAVIEST ELEMENTS

E. K. Hulet\*

University of California, Lawrence Livermore National Laboratory,  
Livermore, CA 94550

## ABSTRACT

We have measured the mass and kinetic-energy partitioning in the spontaneous fission of five heavy nuclides:  $^{258}\text{Fm}$ ,  $^{259}\text{Md}$ ,  $^{260}\text{Md}$ ,  $^{258}\text{No}$ , and  $^{260}\text{No}$  [104]. Each was produced by heavy-ion reactions with either  $^{248}\text{Cm}$ ,  $^{249}\text{Bk}$ , or  $^{254}\text{Es}$  targets. Energies of correlated fragments from the isotopes with millisecond half lives,  $^{258}\text{No}$  and  $^{260}\text{No}$  [104], were measured on-line by a special rotating-wheel instrument, while the others were determined off-line after mass separation. All fissioned with mass distributions that were symmetric. Total-kinetic-energy distributions peaked near either 200 or 235 MeV. Surprisingly, because only a single Gaussian energy distribution had been observed previously in actinide fission, these energy distributions were skewed upward or downward from the peak in each case, except for  $^{260}\text{No}$  [104], indicating a composite of two energy distributions. We were able to fit accurately two Gaussian curves to the gross energy distributions from the four remaining nuclides. From the multiple TKE distributions and the shapes of the mass distributions, we conclude that there is a low-energy fission component with liquid-drop characteristics which is admixed with a much higher-energy component due to closed fragment shells. We now have further evidence for this conclusion from measurements of the neutron multiplicity in the spontaneous fission of  $^{260}\text{Md}$ .

## INTRODUCTION

A central feature of low-energy and spontaneous fission of the heavy elements is the division into fragments of unequal mass. Mass-symmetric fission is a rarer mode, occurring only in two restricted regions of the chart of the nuclides: the Tl to Ac region preceding the actinides, and near the termination of the actinide series of elements. The causes advanced for mass symmetry and asymmetry differ markedly for each region of nuclides. The liquid-drop model describes the broadly symmetric mass distributions and moderate kinetic energies found for the low-energy induced fission of nuclei between Tl and Ac.<sup>1</sup> In contrast, the highly symmetric mass division found in the heaviest Fm isotopes has been ascribed to the strong shell effects emerging near scission from fragments approaching the doubly-magic  $^{132}\text{Sn}$  nucleus.<sup>2,3</sup> Because these fission product nuclei are spherical and stiff toward deformation, the compact configuration at scission

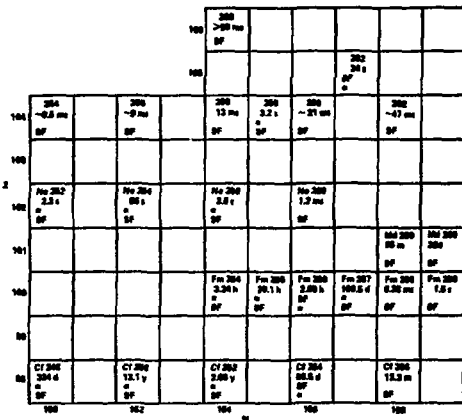
\* Coauthors and collaborators: J. F. Wild, R. W. Lougheed, R. J. Dougan, J. H. Landrum, A. D. Dougan, M. Schädel, R. L. Hahn, P. A. Baisden, C. M. Henderson, R. J. Dupzyk, K. Sümmerer, G. R. Bethune, J. v. Aarle, W. Westmeier, R. Brandt, and P. Patzelt.

MASTER

results in a high Coulomb energy which is translated into unusually large kinetic energies for the fragments. For these nuclides, fragment energies closely approach and some are equal to the Q value for the fission reaction. We have called this "fragment-shell directed" symmetric fission. Previously, these two causes for mass symmetry were thought to be mutually exclusive because they depended on the very different balance between macroscopic forces and single-particle couplings in separate regions of nuclides.

We have gathered evidence from fragment energy measurements in the spontaneous fission (sf) of the heaviest nuclides that strongly suggests symmetric mass division in this region may arise as much from the liquid-drop process as from the influence of emerging fragment shells.<sup>4</sup> We found the total kinetic energy (TKE) distributions of the fragments strongly deviated from the Gaussian distributions which are observed in the fission of lighter actinides. In four of five nuclides studied, the anomalous TKE distribution was skewed sufficiently that it could be decomposed into two Gaussian distributions. From the multiple TKEs and the shapes of the mass distributions, we conclude that there is a lower energy fission component with liquid-drop characteristics which is admixed with a much higher-energy component due to fragment shells. These observations have provided new insights into the fission process which have inspired significant theoretical advances.

#### EXPERIMENTAL



We have measured the energies of coincident fragments arising from the sf of five nuclides with  $Z \geq 100$  and  $N \geq 156$ .<sup>4</sup> A portion of the nuclide chart showing these isotopes and surrounding ones decaying by sf is given in Fig. 1. The very short-lived nuclides, 1.2-ms <sup>258</sup>No (Ref. 5) and 20-ms <sup>260</sup>[104] (Ref. 6), were produced in fusion reactions of 68-MeV <sup>13</sup>C ions with <sup>248</sup>Cm and of 81-MeV <sup>15</sup>N ions with <sup>249</sup>Bk, respectively. Fragment-correlated energy data for these were collected with a new instrument that provides a continuous on-line method for producing short-lived isotopes and measuring the energy of the fragments emitted in sf (Fig. 2). Recoil products emerging from the target were stopped in a band of thin Al foils mounted on the rim of a 30-cm diam wheel that spins up to 5000 rpm. These foils were rotated past opposing banks of trapezoidal-shaped surface-barrier

Fig. 1. Portion of the Nuclide Chart showing isotopes known to decay by sf.

Fig. 2. Recoil products emerging from the target were stopped in a band of thin Al foils mounted on the rim of a 30-cm diam wheel that spins up to 5000 rpm. These foils were rotated past opposing banks of trapezoidal-shaped surface-barrier

detectors, which measured the energies deposited by coincident fragments. With event rates averaging only 5-8 coincident fissions per hour, we obtained 382  $^{258}\text{No}$  sf events together with 59  $^{256}\text{Fm}$  sf events.<sup>7</sup> For  $^{250}\text{[104]}$ , 300 events were recorded along with 41 events from  $^{256}\text{Fm}$  produced by transfer reactions.<sup>8</sup>

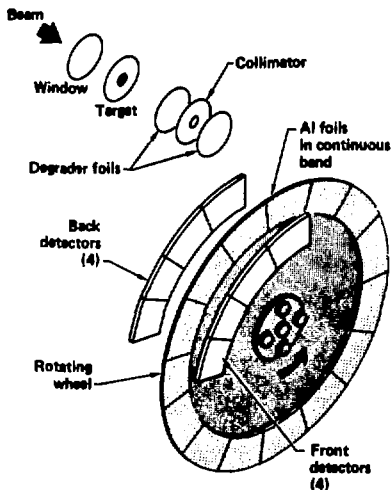


Fig. 2. Schematic diagram of the SWAMI instrument used for measuring coincident fragment energies arising from the sf of millisecond nuclides. A portion of the recoil nuclei produced in the nuclear reactions are stopped in  $100 \mu\text{g}\text{-cm}^{-2}$  Al foils surrounding the rotating wheel, where they are moved between opposing pairs of surface-barrier detectors.

Half-lives of  $^{258}\text{Md}$ ,  $^{259}\text{Md}$ , and  $^{260}\text{Md}$  are sufficiently long to allow time for off-line mass separation for the preparation of isotopically pure sources. These Md isotopes were produced by transfer reactions in bombardments of an  $^{254}\text{Es}$  target with beams of 105-MeV  $^{18}\text{O}$  and 126-MeV  $^{22}\text{Ne}$  from the 88-in cyclotron at the Lawrence Berkeley Laboratory. Recoil products from the bombardments were trapped in Ta foils which were then flown by helicopter from the cyclotron to the Lawrence Livermore National Laboratory for mass separation. Because  $^{256}\text{Fm}$  (157-min sf) is one of the most abundant products of these synthesizing reactions, mass separation was a key technique in freeing  $^{258-260}\text{Md}$  from the massive interference caused by the sf of  $^{256}\text{Fm}$ . The background correction due to this isotope ranged from 8.6% for  $^{259}\text{Md}$  to zero for  $^{260}\text{Md}$ .

The desired mass fraction was collected on an Al foil ( $50 \mu\text{g}\text{-cm}^{-2}$ ) which was subsequently placed between two surface-barrier detectors for the measurement of the correlated fission-fragment energies. The elapsed time between the end of bombardment and the start of counting was 1 h. This short interval was an important factor which allowed

us to study the sf of  $^{259}\text{Md}$  and  $370\text{-}\mu\text{s}$   $^{258}\text{Fm}$ , which is produced by the electron-capture (E.C.) decay of  $60\text{-m}$   $^{258}\text{Md}$ .<sup>9</sup> Fragment energies were determined from calibrations of the detectors with  $^{252}\text{Cf}$  for which we used 181.03 MeV for the average TKE.<sup>10</sup> Fragments that passed through the Al supporting foil were corrected for energy losses amounting to an average of 3.2 MeV. For all of our results, fragment masses were calculated on the basis of the conservation of mass and linear momentum in the fission process.

The sf properties of  $^{258}\text{Fm}$  (Ref. 9,11) had been roughly determined in an earlier study.<sup>3</sup> Previous fission studies had also been made on  $95\text{-min}$   $^{259}\text{Md}$ , which decays directly by sf.<sup>12</sup> In comparison with our older work,<sup>3,12</sup> these re-measurements on mass-separated samples of  $^{258}\text{Fm}$  and  $^{259}\text{Md}$  resulted in more events, much lower contributions from the sf of  $^{256}\text{Fm}$ , and better energy resolution. Because of these improvements, skewing of the TKE distributions became apparent for the first time.

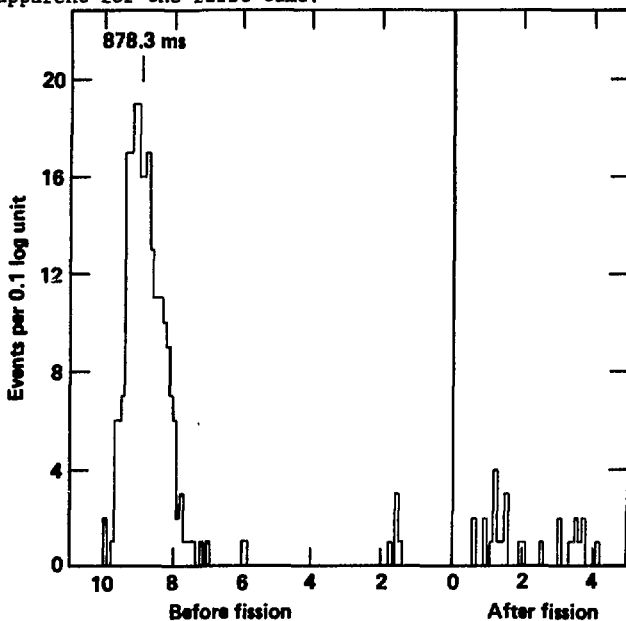


Fig. 3. Logarithmic time distributions for the last energy-windowed photon detected before the sf of  $^{260}\text{Md}$ . The energy window corresponds to the K x-ray region of Fm (112-145 keV).

The longest-lived nuclide,  $^{260}\text{Md}$  with a half-life of 32 d, had been discovered in the A=260 mass fraction after off-line mass separation.<sup>13</sup> Chemical methods have identified a Md isotope as the source of this activity; thus, the Z and A are certain. Although we attribute the decay period to  $^{260}\text{Md}$ , this sf activity could, in prin-

ciple, result from the decay of its possible daughters,  $^{260}\text{No}$  or  $^{260}\text{Fm}$ . These nuclides are expected to have subsecond  $\text{sf}$  half-lives and, therefore, could possibly be in secular equilibrium with the parent  $^{260}\text{Md}$ . We have eliminated  $\beta$  decay to  $^{260}\text{No}$  as a possible source of the observed fissions by measuring the time intervals between 0.04- to 1-MeV betas and subsequent fissions. We found that this time distribution was random and the same as that between any two successive beta particles. Measurements of the time correlation between Fm K or L x-rays and fission events were performed using the same methods and apparatus described in Ref. 9. As shown in Fig. 3 for the spectrum of time intervals between K x-rays and fissions, there are very few photons, except for the random background peak at 878 ms, in the Fm K x-ray energy range occurring before fission. L x-ray time-spectra were similar and demonstrated that branching by E. C. decay to  $^{260}\text{Fm}$  was at most 20%, providing the mean lifetime of  $^{260}\text{Fm}$  is 100 ms or less. Therefore, we ascribe our  $\text{sf}$  results for the A-260 fraction to the direct  $\text{sf}$  of  $^{260}\text{Md}$ .

For the purpose of verifying our bimodal-fission interpretation of the TKE distributions, we have recently measured the multiplicity of prompt neutrons emitted in the  $\text{sf}$  of  $^{260}\text{Md}$  (Ref. 14). Similar to observations from fission in other actinides, we expected an inverse relation between the TKE and the number of neutrons emitted in each event. Because our TKE distribution appeared to be a composite of two distributions, so should the neutron-multiplicity distribution. A small number of neutrons (1 or less) might be expected from fissions with TKEs approaching the Q value of the reaction, whereas the lower-energy TKE peak near 200 MeV should provide a distribution

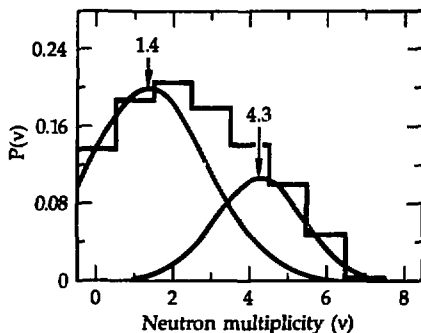


Fig. 4. Neutron multiplicity distribution from the  $\text{sf}$  of  $^{260}\text{Md}$  showing a decomposition into two Gaussian distributions.

comparable with  $^{252}\text{Cf}$  (an average of 3.8 neutrons per fission). Preliminary results from measurements on a single sample are shown in the histogram of Fig. 4. The average neutron multiplicity for this distribution is 2.4 neutrons/fission, which is considerably less than values ranging from 3.5 to 4.15 measured for the heavier actinides. Over 32% of the fissions from  $^{260}\text{Md}$  emit 1 neutron or less; by contrast, only about 2.8% of the fissions from  $^{252}\text{Cf}$  emit 1 neutron or less. We intend to repeat this experiment with the added measurement of fragment energies correlated with the number of neutrons emitted in each fission.

## RESULTS AND DISCUSSION

Figure 5 shows the mass distributions we obtained for the five nuclides. All are symmetric but some more sharply than others. The narrowest, from  $^{258}\text{Fm}$  and  $^{260}\text{Md}$ , have full-widths at half-maximum of 7.5 u while the broadest, that for  $^{260}\text{[104]}$ , is 36 u. In a majority of these nuclides, there are wings extending far outward in mass from the central peak, a feature not so clearly obvious from earlier studies. The fraction of events in these wings is lowest in  $^{258}\text{Fm}$  and  $^{260}\text{Md}$  and increases with Z. A finding common to all these five and to other very heavy nuclides<sup>15,16</sup> is that events with masses residing in these wings are associated with low TKEs while events with TKEs  $\geq 220$  MeV give an exceedingly sharp mass distribution around symmetry. When sf events with TKEs less than 200 MeV are chosen, the resulting mass distributions are very broad and flat. Some might even be characterized as asymmetric if our statistical samples were larger. Thus, we find a low-energy form of fission with very broad mass distributions and a high-energy form associated with sharply symmetric mass division.

In four of the nuclides, the TKE distributions deviated substantially from Gaussian distributions, as seen in Fig. 6. This is a phenomenon not previously observed in the sf of actinide nuclei; for example, the TKE distribution for  $^{240}\text{Pu}$  is given in Fig. 7.<sup>17</sup> Fig. 6

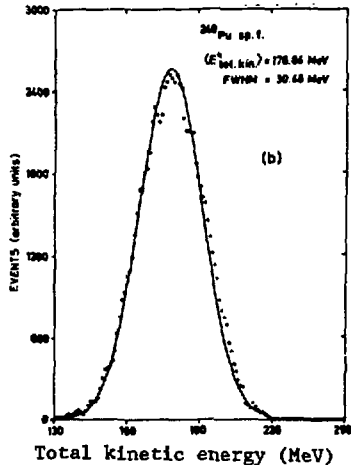


Fig. 7. Gaussian distribution fitted to TKE points for  $^{240}\text{Pu}$  (Ref. 17) A small deviation is seen on the high-energy side of the distribution.

broad TKE and mass distributions obtained for this nuclide, we have interpreted these properties as being characteristic of a liquid-drop

makes it clear that asymmetric tailing from the peak energy can occur toward either higher or lower energies. Furthermore, we note that the peak in each of the TKE curves falls in one of two distinct positions, either near 200 MeV or 235 MeV. Skewing of the TKE curves results in distributing an appreciable portion of the events into each of these two main energy locations. Least-squares fitting of two Gaussian distributions to the TKE curves (e. g., see Fig. 8) gave the following centroids:  $^{258}\text{Fm}$  - 205 and 232 MeV;  $^{259}\text{Md}$  - 201 and 235 MeV;  $^{258}\text{No}$  - 203 and 235 MeV;  $^{260}\text{Md}$  - 195 and 234 MeV. These values were calculated by setting the width of the lower energy Gaussian to the value obtained for  $^{260}\text{[104]}$ .

The sf of  $^{260}\text{[104]}$ , in which the low-energy mode dominates, provides an exception to the largely asymmetric TKE distributions noted above for the other nuclides. Because of the low average TKE and the

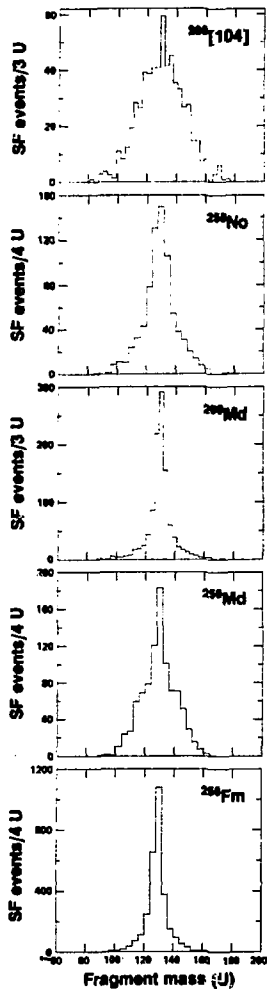


Figure 5. Provisional mass distributions obtained from correlated fragment energies. A small contribution from  $^{256}\text{Fm}$  has been subtracted from most. The mass bins have been chosen to be slightly different for each nuclide.

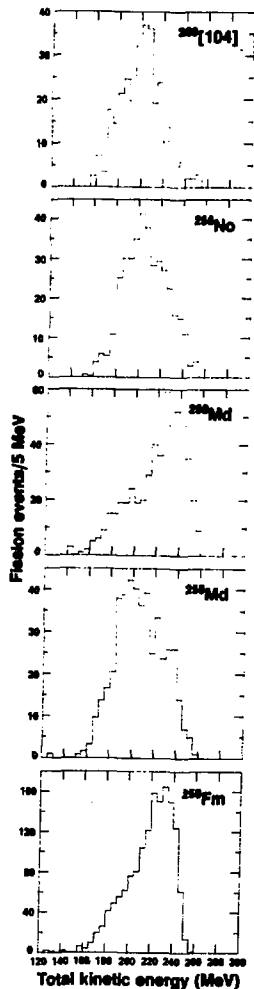


Figure 6. Provisional total-kinetic-energy distributions. A small contribution equivalent to the known amount of  $^{256}\text{Fm}$  has been subtracted from all but the  $^{260}\text{Md}$  distribution.

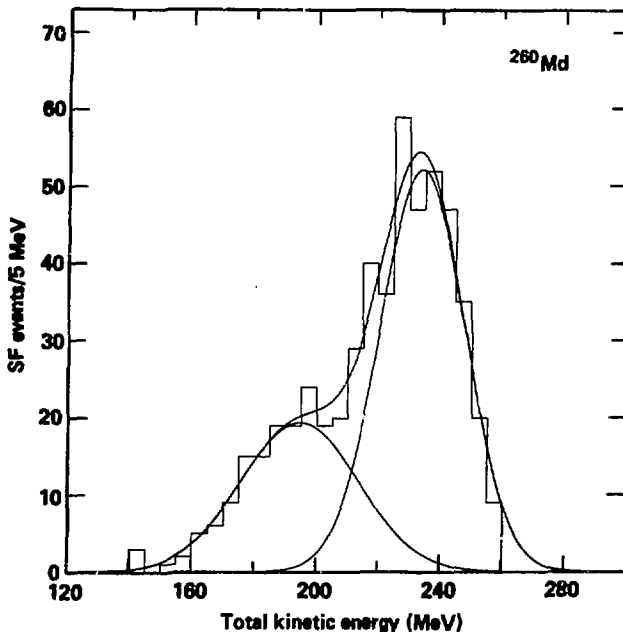


Fig. 8. Decomposition into two components of the asymmetrical TKE distribution measured for  $^{260}\text{Md}$ . A low- and high-energy mode was obtained by fitting with two Gaussian distributions.

mode of fission.<sup>8</sup> The outer asymmetric fission barrier, which may be responsible for asymmetric mass distributions in the fission of all but the heaviest actinides,<sup>18</sup> is predicted to have disappeared below the ground state in  $^{260}[104]$ .<sup>19</sup> Passage through the remaining inner barrier, which contains liquid-drop and shell components, should yield symmetric mass distributions and average TKEs that conform to the estimates of Viola *et al.*<sup>20</sup> Mass symmetry is expected because only reflection-symmetric shapes are allowed by the underlying liquid-drop fission barrier.

Because there are unmistakable high- and low-energy fission distributions occurring concurrently in the same nuclide, we conclude these nuclides sustain two strikingly different modes of fission. We have suggested that the liquid-drop and the "fragment shell" processes are separately responsible for the distinct portions of the TKE distributions.<sup>4</sup> The high-TKE mode depends on the influence of fragment shells which are emerging between the saddle and scission point.<sup>2,3</sup> Fragment shells near the doubly-magic  $^{132}\text{Sn}$  lower the potential-energy path and, thus, guide the mass division toward Sn isotopes near the 82-neutron closed shell. Only the two fission models noted can account for the large ( $\approx 35$  MeV) difference between



the low- and high-energy modes; the symmetric mass distributions, with their disparate widths, are also consistent with these models.

These new observations indicate that symmetric mass division and high TKEs are no longer unique to the heavy Fm isotopes,  $^{258}\text{Fm}$  and  $^{259}\text{Fm}$ . It should be expected that symmetric mass division caused by liquid-drop contributions to the first barrier most likely will extend beyond element-104 toward the region of the "superheavy elements". Even in this unexplored area, exceptionally large TKEs may not be unusual since four of the five nuclides we studied have a significant high-TKE component. In nuclides with neutron numbers approaching 164, high TKEs will be a possibility because symmetric fission leads to spherical fragments containing a closed 82-neutron shell. But as N decreases below 158 neutrons, and Z of the fissioning species increases beyond 100, the opportunity to divide into two Sn fragments diminishes. Within the ranges of Z and N reported here, we observe a trend away from sf characterized by unusually high TKEs and sharply symmetric mass splits and toward the liquid-drop mode represented by  $^{260}\text{[104]}$ . Irrespective of this trend, one of the most striking features is the extraordinarily sharp change in fission properties with the addition of a single nucleon. For instance, adding a proton to  $^{258}\text{Fm}$  or a neutron to  $^{259}\text{Md}$  results in an abrupt inversion in the population of the two fission modes. Such rapid changes are beyond theoretical explanation because the underlying physical parameters tend to vary only smoothly with nucleon numbers.

Earlier,<sup>15</sup> based on having seen a mass-asymmetric mode together with a distinct high-energy, mass-symmetric component in the neutron induced fission of  $^{255}\text{Fm}$ , we had argued strongly for the two-mode hypothesis first proposed by Turkevich and Niday.<sup>21</sup> However, this was not accepted because theoretical calculations of potential-energy surfaces failed to show a hint of two distinct fission paths along such surfaces. Now that our experimental evidence is nearly conclusive, we have suggested there, indeed, must be separate, competitive valleys in the potential-energy surfaces.<sup>4</sup> As a consequence, Broas et al.<sup>22</sup> Müller et al.,<sup>23</sup> Pashkevich and Sandulescu<sup>24</sup>, and Depta et al.<sup>25</sup> have each reported finding several separated paths in the region of the scission point from revised calculations of the potential-energy surface of  $^{258}\text{Fm}$ . One illustration of these newly calculated surfaces is provided in Fig. 9 (Ref. 23), which shows two minimum-energy paths after the first barrier, one leading to a very compact configuration at scission and the other to an elongated, liquid-drop shape. Our experimental TKEs require two different charge separation distances and, therefore, these scission configurations, to reproduce the desired Coulomb energies. Still, all is not well with this picture because there should be nearly equal probabilities of passing through either valley in order to conform to our measurements of the relative amounts of the low- and high-energy modes. The surfaces derived from quasi-static deformations don't provide useful guidance on this point and we feel it will be necessary to introduce dynamical aspects (inertial mass, etc.) to resolve this question.

We thank the staff and operating crew of the 88-in cyclotron for the irradiations. This work was supported by the U. S. Department of Energy under contract No. W-7405-Eng-48.

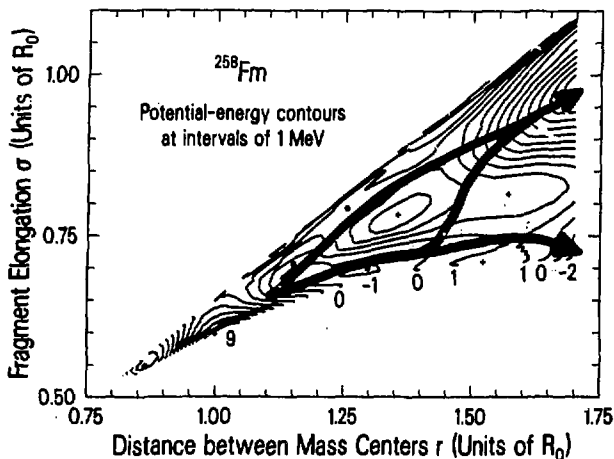


Fig. 9. Potential-energy map of  $^{258}\text{Fm}$  as a function of deformation space (Ref. 23). Two minimum-energy exit channels are indicated.

#### REFERENCES

1. M. G. Itkis *et al.*, *Z. Phys.* **A320**, 443 (1985); V. V. Pashkevich, *Nucl. Phys.* **A162**, 275 (1971); C. Gustafsson, P. Möller, and S. G. Nilsson, *Phys. Lett.* **34B**, 349 (1971); U. Mösel, *Phys. Rev. C* **6**, 971 (1972).
2. U. Mösel and H. W. Schmitt, *Phys. Rev. C* **4**, 2185 (1971); M. G. Mustafa, *Phys. Rev. C* **11**, 1059 (1975).
3. D. G. Hoffman *et al.*, *Phys. Rev. C* **21**, 1972 (1980).
4. E. K. Hulet *et al.*, *Phys. Rev. Lett.* **56**, 313 (1986).
5. M. Nurmi, K. Eskola, P. Eskola, and A. Ghiorso, in Lawrence Berkeley Laboratory Report, Berkeley, CA 94720, UCRL-18667 (1969) p. 63 (unpublished).
6. J. M. Nitschke *et al.*, *Nucl. Phys.* **A352**, 138 (1981); L. P. Somerville *et al.*, *Phys. Rev. C* **31**, 1801 (1985).
7. J. F. Wild *et al.*, *Nucl. Chem. Div. Ann. Report*, Lawrence Livermore National Laboratory, Livermore, CA 94550, UCAR 10062-84/1 (1984), p. 6-23 (unpublished).
8. E. K. Hulet, in *Proceeding of the International School-Seminar on Heavy Ion Physics*, Alushta, 1983 (Joint Institute for Nuclear Research Report D7-83-644, Dubna, USSR, 1983) p. 431.
9. E. K. Hulet *et al.*, *Phys. Rev. C* **34**, 1394 (1986).
10. E. Weissenberger, P. Geltenbort, A. Oed, F. Gönnerwein, and H. Faust, *Nucl. Instrum. & Methods* **A248**, 506 (1986).
11. E. K. Hulet *et al.*, *Phys. Rev. Lett.* **26**, 523 (1971).
12. J. F. Wild *et al.*, *Phys. Rev. C* **26**, 1531 (1982).
13. R. W. Loughhead *et al.*, *J. Less Common Metals*, **122**, 411 (1986).

14. J. F. Wild et al., paper 109, Div. Nucl. Chem. & Tech., 194th National Meeting of the American Chemical Society, New Orleans, Aug. 30-Sept. 4, 1987 (unpublished).
15. R. C. Ragaini, E. K. Hulet, R. W. Lougheed, and J. F. Wild, Phys. Rev. C 9, 399 (1974).
16. H. C. Britt et al., Phys. Rev. C 30, 559 (1984).
17. See, e.g., Fig. 1, A. J. Deruytter and G. Wegener-Penning, in Physics and Chemistry of Fission-1973 (Proc. Symp. Rochester, 1973), IAEA, Vienna (1974), p. 55.
18. P. Möller and S. G. Nilsson, Phys. Lett. 31B, 283 (1970); H. C. Pauli, T. Ledergerber, and M. Brack, Phys. Lett. 34B, 264 (1971); J. Maruhn and W. Greiner, Phys. Rev. Lett. 32, 548 (1974).
19. J. Randrup et al., Phys. Rev. C 13, 229 (1976).
20. V. E. Viola, K. Kwiatkowski, and M. Walker, Phys. Rev. C 31, 1550 (1985).
21. A. Turkevich and J. B. Niday, Phys. Rev. 84, 52 (1951).
22. U. Brosa, S. Grossmann, and A. Müller, Z. Phys. A 325, 242 (1986).
23. P. Möller, J. R. Nix, and W. J. Swiatecki, submitted to Nucl. Phys. A (1986).
24. V. V. Pashkevich and A. Sandulescu, Rapid Communications No.16-86, Joint Institute for Nuclear Research, Dubna, USSR, p 19-23 (1986).
25. K. Depta et al., Mod. Phys. Lett. A 1, 377 (1986).